Rigid Amorphous Fractions and Glass Transitions in Poly(oxy-2,6-dimethyl-1,4-phenylene)†

Jeongihm Pak, Marek Pyda,* and Bernhard Wunderlich

Department of Chemistry, The University of Tennessee, Knoxville, Tennessee 37996-1600, and Chemical Sciences Division, Oak Ridge National Laboratory, Oak Ridge, Tennessee 37831-6197

Received September 16, 2002; Revised Manuscript Received November 20, 2002

ABSTRACT: Semicrystalline poly(oxy-2,6-dimethyl-1,4-phenylene), PPO, is the first example of a polymer that has the glass transition of the rigid amorphous fraction (RAF) above the melting temperature of the crystals. Such phase structure does not allow fast melting below the glass transition and hinders recrystallization. The PPO is analyzed by temperature-modulated differential scanning calorimetry. In the standard DSC of PPO with about 30% crystallinity, a melting peak appears at 515 K, but no glass transition can be seen. The reversing heat capacity of the semicrystalline PPO shows no melting, but a glass transition at about 502 K. Annealing below the beginning of melting causes not only the development of a glass transition as known from amorphous PPO but also a reduction in crystallinity. The RAF was calculated from the deficiency between the measured, reversing heat capacity and the expected thermodynamic heat capacity calculated from our data bank.

Introduction

A recent review of the temperature-modulated differential scanning calorimetry (TMDSC) of semicrystalline polymers has emphasized the importance of the understanding of the nanophase structure in order to describe the thermal properties and establish a link to the molecular structure.[1] The global structure of semicrystalline polymers is that of a metastable system of various nanophases interlocked by molecules which traverse the phases, causing a strong interaction across the interfaces. A nanophase is sufficiently small to show interactions between its opposing surfaces so that it contains practically no bulk material. Polymer nanophases have at least one dimension between 1.0 and 25 nm. At the lower limit, a homogeneous phase, as required by thermodynamics, is not possible because of the atomic nature of matter. Phases of larger dimensions are usually called microphases and still need information about their surfaces for the understanding of their properties. In the visible range, above 1−10 μm, a phase becomes a macrophase which shows only negligible surface effects. Locally, irreversible as well as reversible phase transitions may occur in the overall metastable system of the semicrystalline polymer and can be studied quantitatively by TMDSC.[1]

The types of nanophases in polymers can be characterized as crystalline, amorphous, and intermediate.[2] The intermediate phase can have a separate glass transition temperature from the amorphous phase, T_g(amorphous). Without or with only minimal order, it is called the rigid amorphous fraction (RAF). A RAF was first quantified for poly(oxymethylene), POM, by a comparison between the measured heat capacity, C_p, above the glass transition and the expected C_p calculated using the known liquid and crystalline heat capacities:[3]

$$C_p = w_1C_p(\text{crystal}) + w_2C_p(\text{liquid}) + w_3C_p(\text{RAF}) \quad (1)$$

where w_x is the mass or mole fraction of the corresponding phase. The glass transition of the RAF, T_g(RAF), can fall together with that of the amorphous phase, as is seen, for example, in polyethylene. In this case the only effect of the crystal on the amorphous phase is a broadening of the glass transition region to higher temperature since $w_3 = 0$. Below the glass transition, the intermediate phase has a C_p that is practically identical to C_p(crystal) so that an experimental evaluation by thermal analysis is not possible. In other polymers, T_g(RAF) can be seen between T_g(amorphous) and the melting temperature, T_m, as for example in polypropylene. Most frequently, T_g(RAF) falls together with T_m, as happens also in POM.[3] It will be shown in this paper that T_g(RAF) may even occur above T_m. This special behavior was first suggested for poly(oxy-2,6-dimethyl-1,4-phenylene), PPO, also called poly(oxy-1,4-*m*-xylylene). [4] In this paper the glass and melting transitions of PPO will be described using quantitative, quasi-isothermal TMDSC, and standard DSC as calorimetric tools. Besides a characterization of the glass transition, it will also be shown that the melting has no reversible part, as was recently discovered for many flexible, linear macromolecules.[1]

The crystalline phase of polymers is easily detectable by X-ray diffraction. While the crystallinity can be extracted from the scattering intensity, the size of the crystals can be derived, for example, from the breadth of the diffraction peaks and usually falls into the nanophase region.[5] An interesting observation during TMDSC is that the formation of RAF in poly(3-hydroxy butyrate) goes parallel with the crystal growth and does not form later on cooling.[6] While this conclusion has up to now only been proven for the cited example, it may at least be common on primary crystallization from the melt. In drawn fibers, the RAF was seen to contain a certain amount of cooperative orientation. In these cases, the RAF has a lower enthalpy than the amorphous phase, and an endothermic heat of transition can be observed on disordering. This endotherm may be a considerable fraction of the heat of fusion.[7] In case the RAF is under strain, one should observe an exotherm in the vicinity of the T_g(RAF). This short summary serves as the frame for the discussion of the observed

† This work was presented in part at the 30th NATAS Conference in Pittsburgh, PA, Sept 23−25, 2002.

10.1021/ma021487u CCC: $25.00
Published on Web 12/19/2002

Table 1. Measured and Expected Heat Capacity, C_p, Crystallinity, w_c, and Rigid Amorphous Fraction, w_{RAF}, of Poly(oxy-2,6-dimethyl-1,4-phenylene) at the Given Temperatures[a]

temp, K	C_p(measured), J K^{-1} mol^{-1}	w_c, %	C_p(expected), J K^{-1} mol^{-1}	w_{RAF}, %
488.8	226.8	22.8	246.6	76.5
490.4	227.5	22.7	247.0	76.0
492.5	229.3	22.5	247.7	72.3
494.4	231.0	21.0	248.5	69.8
496.7	233.6	20.2	249.3	63.5
500.7	240.6	12.2	252.3	48.4
504.6	249.9	7.4	254.4	18.9
506.4	253.2	0.0	256.5	14.2
508.7	256.0	0.0	257.0	4.3

[a] The as-received samples were heated to the indicated temperatures, T_0, kept there for 40 min to determine C_p(measured) by quasi-isothermal TMDSC, and then heated to 580 K by standard DSC at 10 K min^{-1} to determine w_c.

behavior of semicrystalline polymers. It also underlines the importance of the detailed, quantitative thermal analysis of semicrystalline polymers by TMDSC as well as standard DSC to find the link between thermal analysis and materials properties.

Experimental Section

A Q1000 system from TA Instruments was used for all new standard DSC measurements, except for the quasi-isothermal analyses which still were done with the Thermal Analyst 2920 system, also from TA Instruments, Inc. Both calorimeters are isoperibol, twin-heat-flux calorimeters with modulation control by the sample temperature sensor. Dry N_2 gas with a flow rate of 20 mL min^{-1} (10 mL min^{-1} for DSC Q1000) was purged through the DSC cell in both instruments. Cooling was accomplished with a refrigerated cooling system (cooling capacity to 220 K). The temperature of the equipment was initially calibrated in the standard DSC mode, using the transition peaks for indium (429.75 K), naphthalene (353.42 K), *n*-octane (216.4 K), acetone (177.9 K), cyclohexane (s/s 186.09 and s/l 297.7 K), cycloheptane (265.1 K), and Sn (505.05 K) at a scanning rate of 10 K min^{-1}. The heat flow was calibrated with the heat of fusion of indium (28.45 J g^{-1}). The onset of melting was determined by extrapolating the sample temperature from the linear portion of the melting peak to the baseline.

The crystallinities in Table 1 were determined from the heat of fusions measured with heating scans at 10 K min^{-1}. Such runs were done after each quasi-isothermal heat capacity measurement for 40 min at the given temperatures.

The quasi-isothermal TMDSC was done with a sinusoidal modulation period of 60 s, a modulation amplitude of 0.5 K, and stepwise temperature increments of the base temperature, T_0, of 2−5 K, depending on the changes expected in the sample response. The last 10 min of the 20 min quasi-isothermal runs was used for data collection to calculate the reversing heat capacity C_p as follows:[8]

$$C_p = \frac{A_\Phi}{A_{T_s}\omega} K' \qquad (2)$$

where A_Φ is the amplitude of the heat flow rate and A_{T_s} is the amplitude of the temperature modulation. Both amplitudes are calculated as the first harmonics of the Fourier series describing the heat flow rate and the sample temperature. The frequency in rad s^{-1} is given by ω, and K' represents the calibration constant at the given conditions of measurement.

The PPO ([O−C_6H_2(−CH_3)$_2$−]$_n$) was purchased from Aldrich Chemical Co., Inc., Milwaukee, WI, in its semicrystalline form. The catalog number is 18,78-1. Its weight- and number-average molar masses are 55 000 and 23 000 Da, respectively. The density is 1.060 mg m^{-3}. Its mechanical and electrical properties are described in the literature.[9]

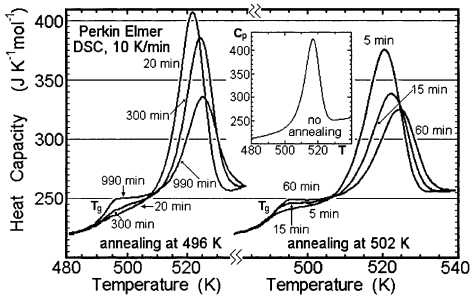

Figure 1. Melting of PPO after various annealing treatments, measured with standard DSC at 10 K min^{-1} to document a higher T_g of the RAF than the crystalline melting temperature.[4]

Samples of 6−15 mg were weighed on a Cahn C-33 electrobalance to an accuracy of ±0.001 mg and encapsulated in standard aluminum pans weighing 23 mg, including the cover with a volume of 38 mm^3. A somewhat lighter reference pan of 22 mg was used for all measurements to correct easily for the asymmetry of the calorimeter by adding the reversing heat capacity from eq 2 for a run with an empty sample pan and the lighter reference pan.[10] Annealing experiments were also done with a Mettler-Toledo standard DSC 8207.[11] In this case the sample mass was similar, but the pan weight was about 56 mg and the pan volume about 95 mm^3.

Results and Discussion

Standard DSC Experiments To Illustrate the RAF Effect in PPO. The apparent heat capacity of the earlier analyzed semicrystalline PPO with a w_c of 0.30% is summarized in Figure 1 with data from standard DSC.[4] The center DSC trace illustrates that the peak temperature of melting is 517 K. As observed before,[12] there is no indication of a glass transition that can be attributed to the noncrystalline material, which is known to occur at about 482 K for amorphous PPO.[13] This was interpreted by us that all the 70% noncrystalline material of the sample is rigid amorphous.[4] Annealing for increasing lengths of time at 496 and 502 K, above the T_g of amorphous PPO, causes a slow development of a glass transition, as can be seen in the left and right traces. The melting peak moves to somewhat higher temperature due to crystal perfection, as expected, but unexpectedly, the crystallinity decreases sharply on annealing. It was concluded from these experiments that the glass transition of the RAF is above the melting temperature of the original crystals and hinders the melting at its zero-entropy-production temperature, which may be 500 K or less. The kinetics of the decrease in crystallinity and RAF was established before between 493 and 505 K.[4]

In the present research, these earlier experiments were repeated on similar samples and analyzed quantitatively by comparison to the heat capacities of solid and liquid of PPO from the ATHAS Data Bank.[14] The crystallinity of the as-received sample was again close to 30%. Figure 2 shows an example of annealing at 503 K. After annealing, the sample was cooled and reheated from 420 to 580 K at 10 K min^{-1} for analysis. A new semicrystalline sample of PPO was used for each run since cooling from the melt does not lead to crystallization, but long exposure to high temperature and showed some indication of decomposition. As before, annealing strongly reduces the crystallinity. The heavy solid line illustrates that after 600 min of annealing no melting peak is left. The glass transitions developed on annealing occur at 486−488 K, slightly above the literature

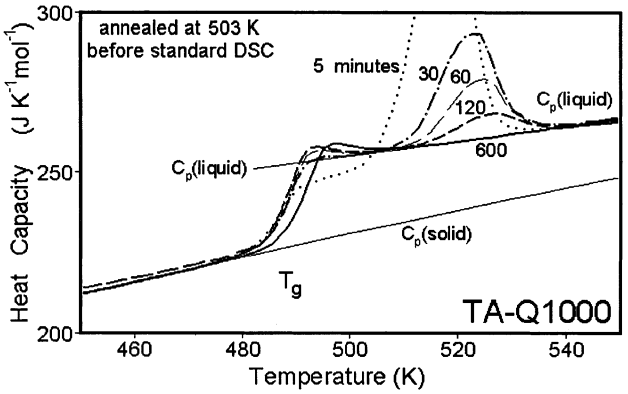

Figure 2. Apparent C_p as measured by standard DSC at 10 K min^{-1} after annealing at 503 K for 5, 30, 60, 120, and 600 min, as indicated.

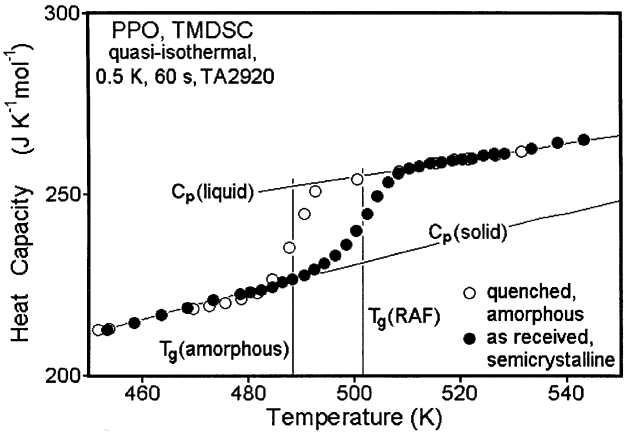

Figure 3. Reversing apparent C_p of as-received, semicrystalline PPO compared to the amorphous sample quenched from the melt on measurements by TMDSC.

value of 482 K for amorphous PPO and the observed value of the sample of Figure 1 of 484 K after quenching from the melt. The long-time annealed sample has an increased value for T_g of 492.8 K. All samples show a small hysteresis peak. The 30−120 min annealed samples have at about 505 K a region almost free of glass transition and melting effects.

The T_g(amorphous) of PPO after annealing at 496 K is almost identical to the standard DSC trace of quenched PPO. Also, at about 500 K, between glass and melting transition, the increase in heat capacity parallels the decrease in crystallinity on annealing. The long-term annealed sample shows in this case no increase in T_g as was seen in Figure 2.

Naturally, a melting below the zero-entropy-production melting temperature would lead to an increase in free enthalpy, forbidden by the second law of thermodynamics. The zero-entropy-production melting temperature is defined in thermodynamics as either the equilibrium melting temperature or, in the case of irreversible processes, the transformation of a metastable crystal into a supercooled melt of the same degree of metastability. The metastability is expressed by the excess in free enthalpy. While polymer crystals supercool when crystallizing from the melt, superheating on melting is a rare event and can usually be avoided.[5] Melting under zero-entropy production is the key technique of thermal analysis to map the free enthalpy of metastable crystals.[5,13]

A possible interpretation of the annealing experiments that does not violate the laws of thermodynamics is as follows: The crystals that melt within the melting peaks of Figures 1 and 2 are superheated. The T_g(RAF) does not occur simultaneously with the melting but actually lies above the true melting temperature. Only as the RAF gains mobility can the melting commence and, as a result, produce more of the mobile amorphous phases, which, in turn, enhances the rate of melting. If there were no hindering by the RAF, the true melting temperature of the present sample would be below 500 K.

The differences in T_g in Figure 2 as well as discrepancies in annealing kinetics seen between the various calorimeters are proposed to result from changes such as decomposition and cross-linking in the amorphous structure on long exposures at high temperature. The measurements with the Perkin-Elmer DSC,[4] and the here and earlier used TA Instrument DSCs,[11] which use similar volume pans, are comparable in all respects. Additional measurements with the Mettler DSC, not included in the present discussion,[11] used larger pan volumes, showed faster annealing kinetics and somewhat lower glass transitions than the other two. Since all calibrations resulted in identical error limits, we must assume that small changes in the amorphous structure occur in different calorimeters. The conclusions reached in all three sets of extensive data, however, are the same, except for small changes in the glass transition and annealing kinetics.

To summarize, the crystalline portions, which are encased in the rigid amorphous fraction, cannot melt as long as T_g(RAF) is not approached, and the melting temperature of the crystalline PPO is not 517 K, as one might deduce from Figure 1, but below 500 K. The glass transition of the RAF, in turn, permits only slow large-amplitude motion in the melting range. It is a well-known fact that about 20 K below T_g some mobility is expected when a time scale of minutes to hours is available. The value of T_g is usually chosen at the temperature of half-devitrification on heating at 1−20 K min^{-1}, the typical DSC operating parameters.[13] More quantitative information about the melting and glass transition of semicrystalline PPO is available from the TMDSC experiments, presented next.

Quasi-Isothermal TMDSC To Separate Glass and Melting Transition Effects. To investigate the glass transition temperature of the RAF in the presence of melting, apparent reversing heat capacities were measured by quasi-isothermal TMDSC on as-received, semicrystalline PPO. For comparison, the same measurements were also carried out on quenched, amorphous PPO. Since at high temperatures PPO may not be sufficiently stable during long-time experimentation as needed for the quasi-isothermal mode, only five temperatures were investigated for any one sample, followed by a check for the absence of mass-loss and decomposition. The results from the multiple samples were then combined to generate the curves as seen in Figure 3. The open circles are for the quenched, amorphous PPO, and the filled circles are for the as-received, semicrystalline PPO. The glass transition is now characteristic of the modulation frequency. The T_g(amorphous) occurs at ≈488 K, while the semicrystalline PPO goes through its broadened glass transition at T_g(RAF) of ≈502 K.

In Figure 4, the apparent reversing heat capacities of the as-received, semicrystalline PPO and the amorphous PPO of Figure 3 are compared to the annealed

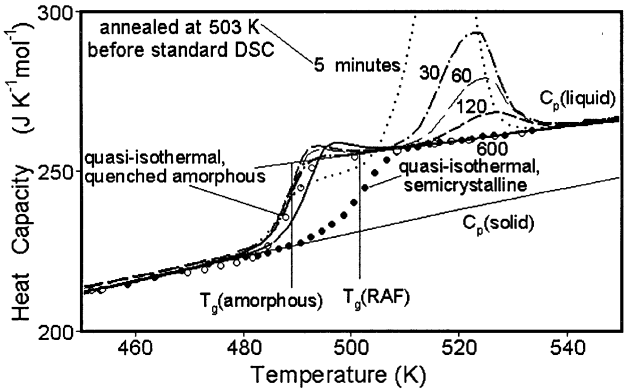

Figure 4. Reversing, apparent C_p of semicrystalline PPO as measured by TMDSC, in comparison to the total heat capacity of Figure 2 measured by standard DSC.

samples displayed in Figure 2. Figure 4 quantitatively supports the interpretation of the melting of PPO being governed by the glass transition of the RAF. The observed melting peaks in Figures 1 and 4 are not only broadened due to instrument lag[15] but also affected by the intervention of the glass transition of the RAF.

Another unexpected result from inspection of Figure 4 is the complete absence of a reversing contribution to the melting of the semicrystalline PPO. All flexible macromolecules reviewed recently[1] show at least a small amount of reversible melting, which was linked to the partial melting by some molecules. The more rigid PPO, and possibly also a polycarbonate,[6] do not follow this trend. A more detailed investigation of this difference between flexible and rigid macromolecules is now possible with TMDSC and may shed more light on their crystallization mechanisms.

Without annealing, the quasi-isothermal TMDSC of the semicrystalline PPO in Figure 3 shows only little overlap with the low-temperature glass transition of the quenched PPO. This proves that there is no bulk amorphous fraction in the as-received, semicrystalline PPO at low temperature. The RAF makes up all of the noncrystalline material, as assumed before.[4] The glass transition of the RAF is independent of the bulk material, as one would expect for nanophases. The T_g of amorphous PPO shown in Figure 4 is almost identical to the semicrystalline PPO after annealing at 503 K.

Combined TMDSC and DSC To Evaluate the Change of RAF during Melting. In a final set of experiments, the as-received, semicrystalline PPO samples were modulated for 40 min at a series of given temperatures, T_0, as listed in Table 1 for the measurement of the reversing C_p(measured). After the modulation, these samples were immediately heated to 580 K under standard DSC conditions to obtain the changing crystallinities, w_c, which are also listed in Table 1. From this comparison, it is clear that the rigid amorphous fraction restricts the melting of the crystals. At the lowest temperatures, the decrease in crystallinity is small for the 40 min isotherm. As soon as the temperature reaches the glass transition temperature of the RAF, determined to be 502 K in Figure 3, the melting peak decreases drastically.

From the crystallinities listed in Table 1, an expected C_p is calculated. The solid heat capacity represents the crystalline phase, while both amorphous phases are initially assumed to be represented by the heat capacity of the liquid phase. Figure 5 shows with the open circles the expected C_p for the entries in Table 1. The filled

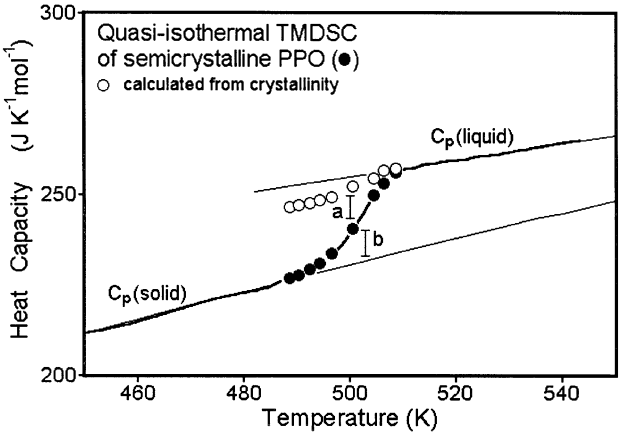

Figure 5. Expected and measured C_p of semicrystalline PPO (data of Table 1).

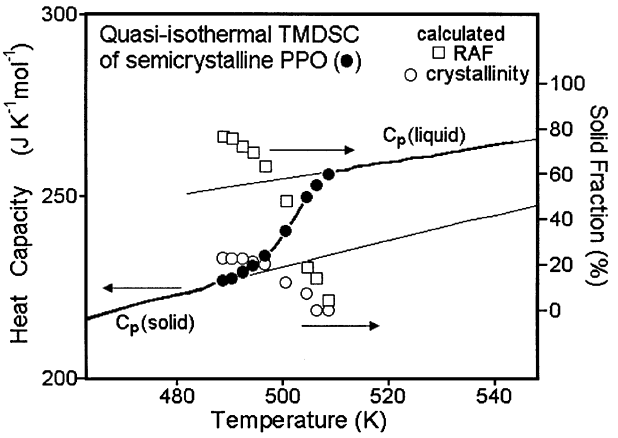

Figure 6. Rigid amorphous fraction and w_c of semicrystalline PPO based on Figure 5.

circles are the C_p(measured) determined by quasi-isothermal TMDSC before the crystallinity determination. It is also given in Table 1. The reversing C_p-(measured) is similar to the results on semicrystalline PPO in Figure 3.

The deficiency between C_p(expected) calculated assuming a fully mobile amorphous phase and C_p(measured) is marked as the length a in Figure 5. The length b is then due to the RAF which has already gone through its glass transition in the time scale of the experiment and the amount of crystal already melted. The ratio a to ΔC_p, the difference between C_p of the liquid and the solid, is the remaining RAF, w_{RAF}, in the semicrystalline PPO at the given temperature. The w_{RAF} at 489 K is about 76% and decreases to 4% at 509 K. The difference between the measured C_p and the solid C_p, in turn, marked as b in Figure 5, is the mobile amorphous fraction when divided by ΔC_p.

In Figure 6, the crystallinity, w_c, and the RAF, w_{RAF}, are plotted together with the measured heat capacity for the samples of Table 1 and Figure 5. As the temperature increases, the crystallinity and the RAF decrease, but at different rates. The mobile amorphous fraction given by $b/\Delta C_p$ from Figure 5 reaches 100% at about 510 K. Up to about 495 K the crystallinity decreases very little, while the RAF loses almost 20% of its value, which is in accord with the assumption that the surrounding glass must become mobile before melting can occur. Between 495 and 510 K the decrease of both the RAF and the crystallinity is close to linear, with the RAF losing three times as much solid fraction as

the crystallinity. Once major melting has started, these rates of devitrification and melting stay practically constant until all RAF and crystallinity go to zero at about the same temperature (≈510 K).

Conclusions

This research calls attention to the importance of the RAF in the understanding of the complicated nanophase structure of semicrystalline polymers. The global structure is metastable with the crystals interconnected by the much longer molecules. Local reversible and irreversible transitions can occur within this global structure. In most polymers, the noncrystalline phase can be separated into at least two nanophases: a mobile and a rigid amorphous fraction. For PPO, the RAF makes up practically all the noncrystalline phases, and its glass transition temperature lies above the melting transition and prohibits melting before sufficient mobility is reached within the RAF. Coupling reversing heat capacities by TMDSC and total apparent heat capacities by DSC permits a quantitative assessment of the transitions. The RAF needs to become mobile before melting can begin. Once melting has begun, the decrease in RAF for a given amount of melting seems to be constant at 3% RAF for 1% crystallinity.

The reverse process is the formation of RAF on crystallization. As mentioned above, at least for PHB, a parallel growth of crystallinity and RAF was observed. Furthermore, a restriction of the crystallization is expected on formation of RAF when T_g(RAF) is close to the melting or crystallization temperature. If the RAF has a glass transition above the melting temperature, as in PPO, crystal growth must stop when a given, nanometer-size crystal is reached. This should be the reason for the difficulty of crystallization of PPO from the melt which can be removed by addition of a plasticizer or crystallization from solution. A polymer that seems to have a T_g(RAF) below the cold-crystallization temperature seems to be poly(butylene terephthalate). In this case only a very small crystallinity could be grown below the T_g(RAF), which is at about 320 K, and T_m is 518 K.[16]

Of additional interest is that in this analysis no reversible melting of the PPO was found by TMDSC. It may be that the reversible melting is restricted to the more mobile polymers with glass transitions far below the melting transition.

Acknowledgment. This work was supported by the Division of Materials Research, National Science Foundation, Polymers Program, Grant DMR-9703692, and the Division of Materials Sciences, Office of Basic Energy Sciences, U.S. Department of Energy at Oak Ridge National Laboratory, managed and operated by UT-Battelle, LLC, for the U.S. Department of Energy, under Contract DOE-AC05-00OR22725.

References and Notes

(1) Wunderlich, B. *Prog. Polym. Sci.* **2003**, *28*, 383−450.
(2) Chen, W.; Wunderlich, B. *Macromol. Chem. Phys.* **1999**, *200*, 283.
(3) Suzuki, H.; Grebowicz, J.; Wunderlich, B. *Br. Polym. J.* **1985**, *17*, 1.
(4) Cheng, S. Z. D.; Wunderlich, B. *Macromolecules* **1987**, *20*, 1630.
(5) Wunderlich, B. *Macromolecular Physics;* Academic Press: New York, 1973−1980; Vols. 1−3.
(6) Schick, C.; Wurm, A.; Mohammed, A. *Colloid Polym. Sci.* **2001**, *279*, 800.
(7) Kwon, Y. K.; Boller, A.; Pyda, M.; Wunderlich, B. *Polymer* **2000**, *41*, 6237.
(8) Wunderlich, B.; Jin, Y.; Boller, A. *Thermochim. Acta* **1994**, *238*, 277.
(9) *Encyclopedia of Polymer Science and Engineering*; John Wiley & Sons: New York, 1988; Vol. 13.
(10) Boller, A.; Okazaki, I.; Ishikiriyama, K.; Zhang, G.; Wunderlich, B. *J. Therm. Anal.* **1997**, *49*, 1081.
(11) Pak, J.; Pyda, M.; Wunderlich, B. *Proc. 30th NATAS Conf. in Pittsburgh, PA*, Sept 23−25; Kociba, K. J., Kociba, B. J., Eds.; **2002**, *30*, 345−350.
(12) Karasz, F. E.; Bair, H. E.; O'Reilly, J. M. *J. Polym. Sci., Part A-2* **1968**, *6*, 1141.
(13) Turi, E., Ed.; *Thermal Characterization of Polymeric Materials*; Academic Press: New York, 1997.
(14) Gaur, U.; Wunderlich, B. *J. Phys. Chem. Ref. Data* **1981**, *10*, 1038.
(15) Boller, A.; Ribeiro, M.; Wunderlich, B. *J. Therm. Anal. Calorim.* **1998**, *54*, 545.
(16) Cheng, S. Z. D.; Pan, R.; Wunderlich, B. *Makromol. Chem.* **1988**, *189*, 2443.

MA021487U